5. ANKARA INTERNATIONAL AEROSPACE CONFERENCE **AIAC-2009-036**
17-19 August 2009 - METU, Ankara TURKEY

INVISTIGATION OF TURBULENCE MODLING TO SIMULATION OF THE GROUND EFFECT

M. H. Djavareshkian[1]
Ferdowsi University of Mashhad
Mashhad, Iran

A. Parsania[2]
Ferdowsi University of Mashhad
Mashhad, Iran

ABSTRACT

A pressure-based is procedure to solving Navier Stokes equations on a nonorthogonal mesh with collocated finite volume formulation is developed for incompressible flows. The procedure incorporates several eddy-viscosity turbulence models for simulation of the ground effect. The aim of the present study is to investigate the effect of turbulent models on the simulation of the ground effect. In this study, the effect of the moving boundary is assessed. The results of this simulation around the airfoil-NACA 0015-are compared with experimental data. Computation visualization of the flows shows that the turbulent models have more effect on the simulation and the moving boundary is effect when the ground clearance is small.

INTRODUCTION

The transportation system using ground effect is expected to become one of high speed and efficient transportation systems. Wing-in-ground-effect (WIG) vehicles are very efficient, which helps to increase the flight range at a reduced specific fuel consumption compared with the conventional aircraft. One of the new transportation system using ground effect, is call “Aero-Train”. Aero-Train has wings and flies near the ground inside a guide way using ground effect.

There have been successful investigations on the aerodynamics of airfoil and wing in close proximity to ground. Hee Jung Kim et al [1] investigate aero numeric optimal design of a wing-in-ground-effect craft and found optimum shape for component of wing-in-ground-effect (WIG) vehicles. Ahmed and Sharma [2] performed an experimental investigate and found the effect of variation of angle of attack and ground clearance on aerodynamic characteristics of symmetrical airfoil NACA 0015. Robert E. Curry [3] investigated about the dynamic parameters of a cranked arrow Wing Airplane in ground effect. K. H. Jung and et al [4] make experiment and study about the effect of aspect ratio and endplate on aerodynamic characteristic of wing in ground effect. L. K. Kliment and K. Rokhsaz [5] investigate wake vortices of air craft in ground Effect. Numerical simulation and studies of aerodynamic parameters about ground effect phenomena has been performed by J. L. Smith [6], Patrick Vu [7], A. H. Melvin [8].

In all of the above numerical studies, the effect of the turbulence modeling has been not assessed. Also in actual problem the ground is moving while in experimental tests, ground is fixed.

The objection of the this research, is to investigate about turbulence modeling in ground effect phenomena also since in actual problem the ground is moving and in experimental test the ground is fixed, the effect of moving ground has been investigated.

[1] Associated prof. in Department of Mechanical Engineering, Ferdowsi of Mashhad university, Mashhad, Iran, Email: javareshkian@ferdowsi.um.ac.ir

[2] Master of Science student, in Department of Mechanical Engineering, Ferdowsi of Mashhad university, Mashhad, Iran, Email: ahmad.parsania@gmail.com

FINITE VOLUME DISCRETIZATION

The basic equations, which describe conservation of mass, momentum and scalar quantities, can be expressed in the following vector form, which is independent of used coordinate system.

$$\frac{\partial \rho}{\partial t} + \mathrm{div}(\rho \vec{\mathbf{V}}) = S_m$$

(*1*)

$$\frac{\partial(\rho \vec{\mathbf{V}})}{\partial t} + \mathrm{div}(\rho \vec{\mathbf{V}} \otimes \vec{\mathbf{V}} - \vec{\mathbf{T}}) = \vec{\mathbf{S}}_v$$

(2)

$$\frac{\partial(\rho \phi)}{\partial t} + \mathrm{div}(\rho \vec{\mathbf{V}} \phi - \vec{\mathbf{q}}) = \vec{\mathbf{S}}_\Phi$$

(3)

Where ρ, $\vec{\mathbf{V}}$ and ϕ are density, velocity vector and scalar quantity respectively, $\vec{\mathbf{T}}$ is the stress tensor and $\vec{\mathbf{q}}$ is the scalar flux vector. The latter two are usually expressed in terms of basic dependent variables. The stress tensor for a Newtonian fluid is:

$$\vec{\mathbf{T}} = -(P + \frac{2}{3}\mu\, \mathrm{div}\, \vec{\mathbf{V}})\vec{\mathbf{I}} + 2\mu \vec{\mathbf{D}}$$

(4)

and the Fourier-type law usually gives the scalar flux vector:

$$\vec{\mathbf{q}} = \Gamma_\phi\, \mathrm{grad}\Phi$$

(5)

For the purpose of illustration (3) may be expressed in 2D Cartesian coordinates as:

$$\overbrace{\frac{\partial(\rho\phi)}{\partial t}}^{\text{transient term}} + \overbrace{\frac{\partial(\rho u \phi)}{\partial x} + \frac{\partial(\rho v \phi)}{\partial y}}^{\text{convection term}} - \overbrace{\frac{\partial}{\partial x}(\Gamma_\phi \frac{\partial \phi}{\partial x}) - \frac{\partial}{\partial y}(\Gamma_\phi \frac{\partial \phi}{\partial y})}^{\text{diffusion term}} = \overbrace{S_\phi}^{\text{source}}$$

(6)

Integration of (6) over a finite volume (see e.g. Figure. 1) and application of the Gauss divergence Theorem yield a balance involving the rate of change in ϕ, face fluxes and volume-integrated net source. The discretized equations resulting according to SIMPLE algorithm take the form:

$$A_P.\phi_P = \sum_{m=E,W,N,S} A_m.\phi_m + S'_\phi$$

(7)

Where A's are the convection-diffusion coefficients. The term S'_ϕ in Eq. (7) contains quantities arising from non-orthogonality, numerical dissipation terms, external sources, deferred correction terms, and $(\rho\delta\upsilon/\delta t)\phi_P$ of the old time-step/iteration level. For the momentum equations it is easy to separate out the pressure-gradient source from the convected momentum fluxes.

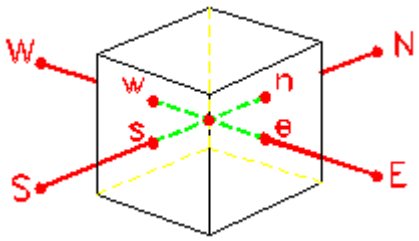

Figure 1: *Finite volume and storage arrangement*

RESULTS

In this paper the main emphasis is concentrated on the simultiaon of incompressible flow around the airfoil close the ground. Computational results are shown in followed figures for a baseline series of test cases.

Figure 2 shows grid independenc of computational domain.Three grids have been used with number of cells 90×50 and 300×120 and 450×120 that second grid is chosen.

Figure 3 represent the comparison of pressure distribution on the upper and lower surface for free streem and three ground clearance.this show that in the low ground clearance, pressure coefficient on pressure side of the airfiol increase because of air cushion on the lower surface of airfoil.this phenomena lead to increase the lift force of wing in ground effect.

Figure 4 shows the pressure distribution on the upper and lower surface of the airfoil for an angle of attack 10° and h/c=0.05 for different turbulent modling. This comparison shows that the spalart and allmaras model and Reynols stress model under estimate in both suction side and pressure side. Altogether $k-\varepsilon$ model more adapt with experimental data.

Figure 5 shows the pressure distribution on the upper and lower surface of the airfoil for an angle of attack 10° and h/c=0.2 for different turbulent modling. This comparison shows that the spalart and allmaras model is over estimate in pressure side and under estimate in suction side. The $k-\varepsilon$ model and Reynols stress show the better comparison with experimental data in the pressur side. in suction side, two mention models under estimate pressure distribution. Altogether $k-\varepsilon$ and Reynols stress model more adapt with experimental data.

Figure 6-7 represent the effect of moving and fixed ground. This comperison shows that the effect of moving grond in the small ground clearance is considerable and in high ground clearance there is not difference between moving an fixed ground and altogether is not important factor.

Figure 8-9 represent the contours of velocity magnitude for moving and fixed ground for an angle of attack 10° and h/c=0.05.

Figure 10-11 represent vector of velocity of wake flow field behind the trailing edge of airfoil for angle of attack 10°, h/c=0.05 and two boundary conditions.As it can be seen, the velocity profile shape near ground is different for two boundaries.

Conclusions

İn the numerical simulation of flow around the airfoil in ground effect, pressure distribution on the upper and lower surface is depend on turbulent modling. For three turbulent modling $k-\varepsilon$ model, Reynols stress model and spalart and allmaras model, $k-\varepsilon$ model is more adapt with experimental data.

Moving ground influence pressure distribution on the airfoil surface in low ground clearance, but it is not considerable parameter.

References

1- Kim, H. J., and Chun, H. H., and Jung, K. H., *Aero numeric optimal design of a wing-in-ground-effect craft*, J Mar Sci Technol, 2008.

2- Ahmed, M.R., and Sharma, S. D., *An investigation on the aerodynamics of a symmetrical airfoil in ground effect*, Experimental Thermal and Fluid Science, p: 633–647, 2005.

3- Robert, E. C., *Dynamic Ground Effectfor a Cranked Arrow Wing Airplane*, NASA Technical Memorandum, 1997.

4- Jung, K. H., and Chun Hee, H. H., and Kim, J., *Experimental investigation of wing-in-ground effect with a NACA6409 section*, J Mar Sci Technol, 2008.

5- Linda, K., and Kliment., and Rokhsaz, K., *Experimental Study of Aircraft Wake Vortices in Ground Effect*, Department of Aerospace Engineering, College of Engineering, Wichita State University, Wichita, Kansas, 67260-0044, USA.

6- Smith, J. L., *Computational Analysis of Airfoils in Ground Effect For Use as a Design Tool*, Msc Thesis, Department of Mechanical and Aerospace Engineering Morgantown, West Virginia, 2007.

7- Vu Patrick, *CFD study of wing tip vortices for inverted airfoils in ground effect*, MSc thesis, School of engineering, School of engineering, September 2006

8- Melvin, A. H., *Simulation-Based Aerodynamic Design of High-Lift Devices in Ground Effect*, Ph.D Thesis, Department of Mechanical and Aerospace Engineering, Princeton University, 2007.

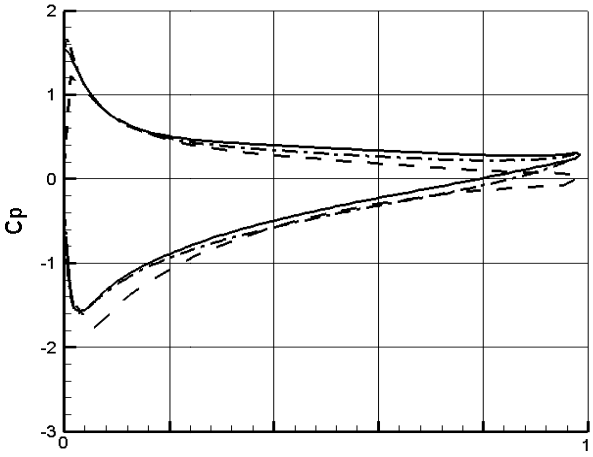

Figure 2: *Pressure distribution on the surface of the airfoil for an angle of attack 10 ^{o} and h/c=0.05 for* $90\times50 grid$ ▬ ▬ ▬ , $300\times120 grid$ ▬▬▬ , $450\times120 grid$ ▬ · ▬ · .

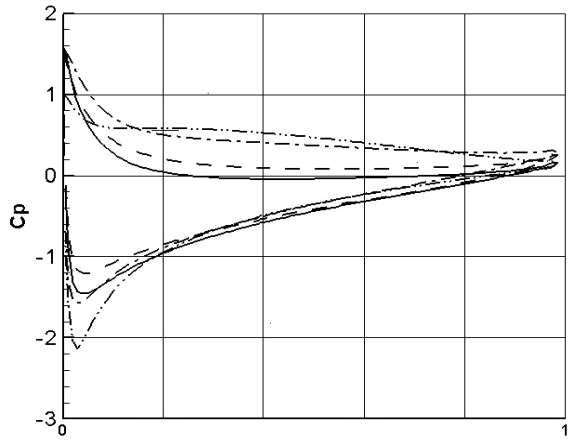

Figure 3: *Pressure distribution on the surface of the airfoil for an angle of attack 10 and* $k-\varepsilon$ *model. infinity* ▬▬▬ , *h/c=0.8* ▬ ▬ , *h/c=0.2* ▬ · ▬ , *h/c=0.05* ▬ · · .

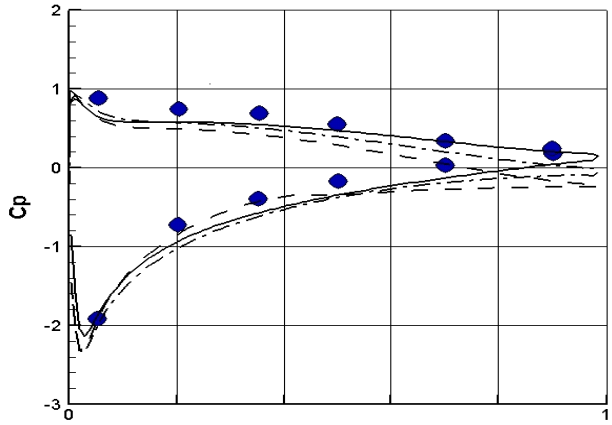

Figure 4:*Pressure distribution on the surface of the airfoil for an angle of attack 10 ^{o} and h/c=0.05, experimental* ●, $k-\varepsilon$ ▬▬▬ , *RSM* ▬ ▬ · , *SA* ▬ · ▬ .

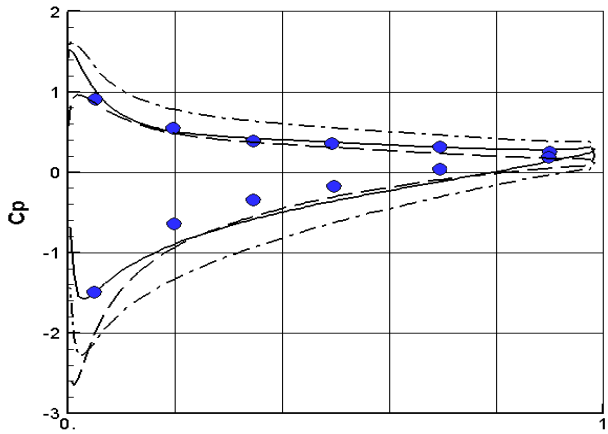

Figure 5:*Pressure distribution on the surface of the airfoil for an angle of attack 10 ^{o} and h/c=0.2, experimental* ●, $k-\varepsilon$ ▬▬▬ , *RSM* ▬ ▬ · , *SA* ▬ · ▬ .

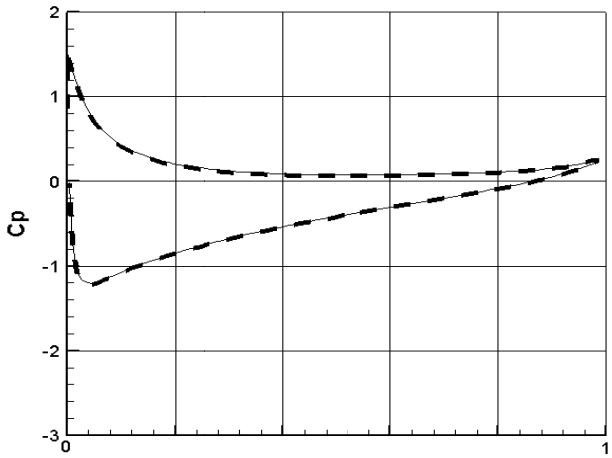

Figure 6: *Pressure distribution on the surface of the airfoil foran angle of attack 10 ^{o} and h/c=0.8 for* $k-\varepsilon$ *model.*
Fixed surfa ▬▬▬ ,*Moving surface* ▬ ▬ ▬ .

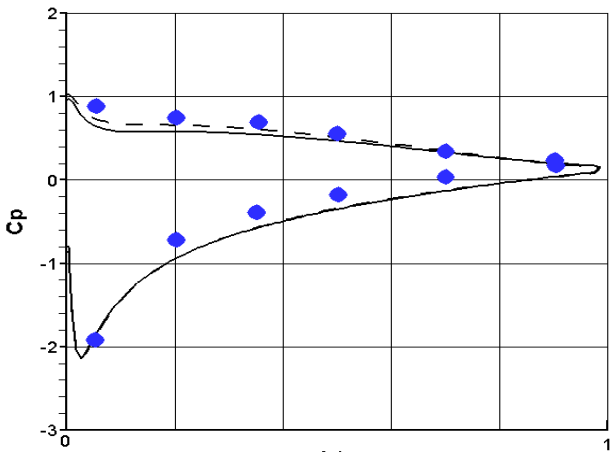

Figure 7: *Pressure distribution on the surface of the airfoil for an angle of attack 10 ^{o} and h/c=0.05 for* $k-\varepsilon$ *model. experiment* ●, *fixed surface* ▬▬▬ , *moving surface* ▬ ▬ ▬ .

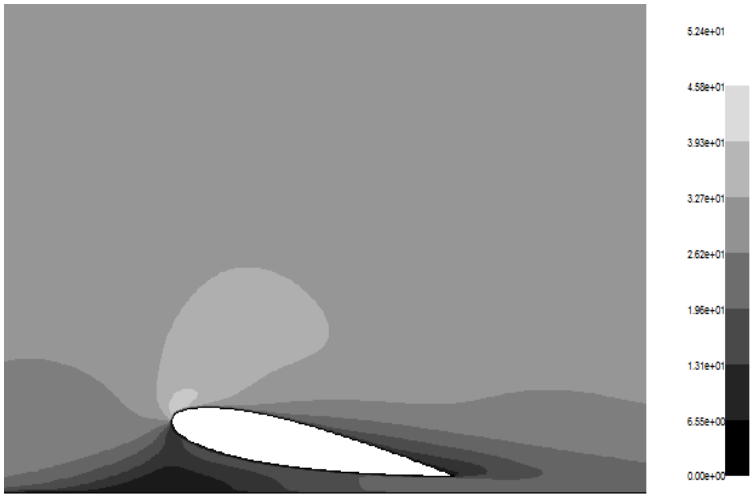

Figure 8: *Contours of velocity magnitude for angle of attack 10° and h/c=0.05 and fixed boundary*.

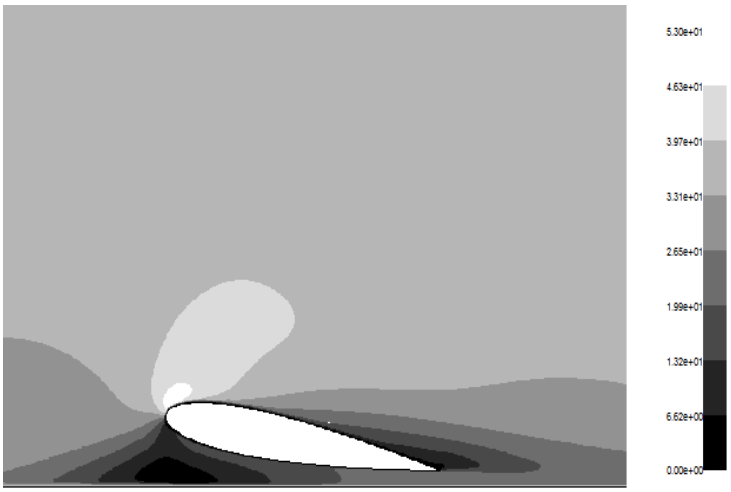

Figure 9: *Contours of velocity magnitude for angle of attack 10° and h/c=0.05 and moving boundary.*

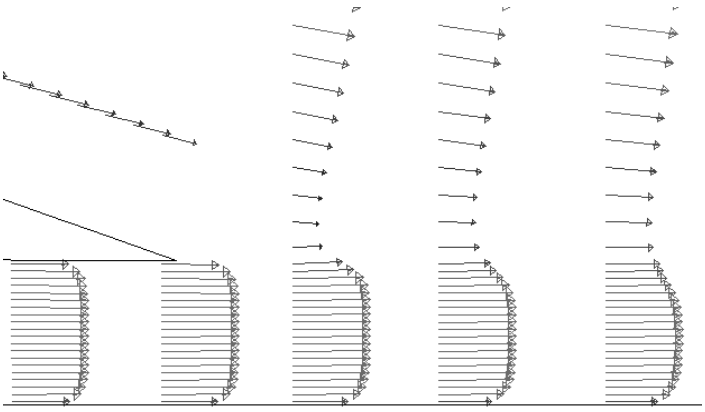

Figure 10: *Vector of velocity of wake flow field for angle of attack 10° and h/c=0.05 and fixed boundary*.

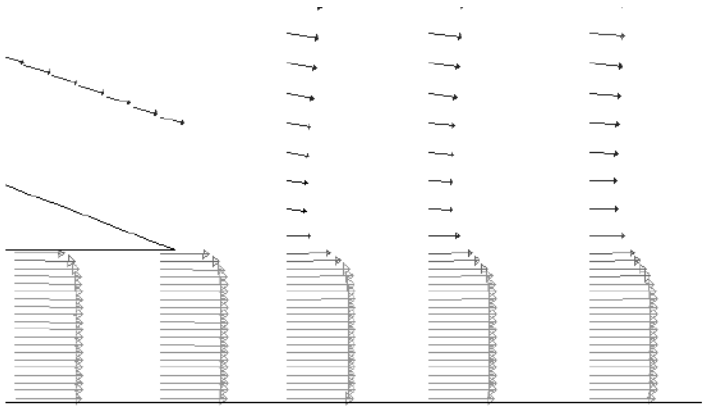

Figure 11: *Vector of velocity of wake flow field for angle of attack 10° and h/c=0.05 and moving boundary.*